

Supporting Information

Preparations:

General Procedures and Materials: All chemicals and solvents in the synthesis were reagent grade and used as received. $\text{Ti}[\text{Tp}^{\text{Me,mt4}}]$ and the Mn Schiff base were prepared according to the literature.^{s1,s2}

(PPh₄)[(Tp^{Me,mt4})Fe(CN)₃]•H₂O: $\text{Ti}[\text{TpMe,mt4}]$ (0.31 g, 0.50 mmol) in dichloromethane (40 mL) was mixed with KCN (0.10 g, 1.5 mmol) in MeOH (40 mL). To $\text{FeCl}_3 \cdot 6\text{H}_2\text{O}$ (0.14 g, 0.50 mmol) in MeOH (100 mL) slowly added the mixture, turning a brown solution. After stirring for 5 h, white solids (TiCl) were precipitated, which was filtered off. The resulting solution was treated with PPh_4Cl (0.30 g) and heated at 80 °C for 5 h. The filtered solution was evaporated to a small amount and ether was added to obtain brown solid. The product was washed with water several times and dried in air. Yield: 77%. IR data of $\nu(\text{CN})$: 2115cm^{-1} . Elemental analysis (%) calcd for $(\text{PPh}_4)[(\text{Tp}^{\text{Me,mt4}})\text{Fe}(\text{CN})_3] \cdot \text{H}_2\text{O}$: C 68.77, H 6.11, N 14.15; found : C 68.69 , H 6.08, N 14.32.

$[(\text{Tp}^{\text{Me,mt4}})\text{Fe}(\text{CN})_3]_2[\text{Mn}(\text{L})]_2$ (1): $[\text{Mn}(\text{L})(\text{H}_2\text{O})]\text{Cl}$ (18 mg, 0.040 mmol) in MeOH/MeCN (10 mL, v/v 1:1) was added to $(\text{PPh}_4)[(\text{Tp}^{\text{Me,mt4}})\text{Fe}(\text{CN})_3] \cdot \text{H}_2\text{O}$ (35 mg, 0.040 mmol) in MeOH/MeCN (10 mL, v/v 1:1). The resulting solution was stirred for a few minutes and filtered. The brown solution was slowly evaporated in the dark, affording brown crystals in 2 days. Yield: 10%. Elemental analysis (%) calcd for $\text{C}_{92}\text{H}_{104}\text{B}_2\text{Br}_4\text{Fe}_2\text{Mn}_2\text{N}_{22}\text{O}_4$: C 51.52, H 4.89, N 14.37; found: C 51.51, H 4.83, N 14.49.

(s1) A. L. Rheingold, L. M. Liable-Sands, S. Trofimenko, *Inorg. Chem.*, 2000, **29**, 1333.

(s2) R. Karmakar, C. R. Choudhury, G. Bravic, J. -P. Sutter, S. Mitra, *Polyhedron*, 2004, **23**, 949.

Physical Measurements:

Elemental analyses for C, H, and N were performed at the Elemental Analysis Service Center of Sogang University. Infrared spectra were obtained from KBr pellets with a Bomem MB-104 spectrometer. Magnetic susceptibilities for **1** were carried out using a Quantum Design SQUID susceptometer (dc) and a PPMS magnetometer (ac). Diamagnetic corrections of all samples were estimated from Pascal's Tables.

Crystallographic Structure Determination:

Single crystal of **1** was taken with a cryoloop and mounted on a goniometer head in a cold stream of liquid nitrogen. The diffraction data were measured with synchrotron radiation on a 6B MX-I ADSC Quantum-210 detector with a silicon (111) double-crystal monochromator at the Pohang Accelerator Laboratory, Korea. The ADSC Quantum-210 ADX program (Ver. 1.92) was used for data collection and HKL2000 (Ver. 0.98.699) was used for cell refinement, reduction, and absorption correction. The structures were solved by direct methods and refined by full-matrix least-squares analysis using anisotropic thermal parameters for non-hydrogen and non-disordered atoms with the SHELXTL program. Lattice solvent molecules are significantly disordered and could not be modeled properly, thus the program SQUEEZE, a part of the PLATON package of crystallographic software, was used to calculate the solvent disorder area and remove its contribution to the overall intensity data. The contributions of some 66 electrons were removed from the unit-cell contents, and as $Z = 1$ in this case, this could/might correspond with the removal of solvent such as 1.5(MeOH) and 1.5(MeCN) [some 60 electrons] from the $\text{Fe}^{\text{III}}_2\text{Mn}^{\text{III}}_2$ formula unit. The carbon atoms (C24A, C24B, C25A, C25B, C30A, and C30B) were disordered over two sites (0.5: 0.5 for C24A-C25A and C24B-C25B; 0.71: 0.29 for C30A and C30B) and these atoms only were isotropically refined using PART. All hydrogen atoms except for hydrogens bound to the atoms (C28, C29, C30A, and C30B), in which the ethylene C28 and C29 were not disordered but the methyl carbon C30A and C30B linked to C28 and C29 were disordered, were calculated at idealized positions and refined with the riding models. Crystal data of **1** ($\text{C}_{92}\text{H}_{104}\text{B}_2\text{Br}_4\text{Fe}_2\text{Mn}_2\text{N}_{22}\text{O}_4$): Mr = 2144.81, triclinic, space group $P-1$, $a = 12.414(3) \text{ \AA}$, $b = 14.003(3) \text{ \AA}$, $c = 15.544(3) \text{ \AA}$, $\alpha = 98.07(3)^\circ$, $\beta = 105.42(3)^\circ$, $\gamma = 98.98(3)^\circ$, $V = 2525.6(9) \text{ \AA}^3$, $Z = 1$, $D_{\text{calc}} = 1.410 \text{ cm}^{-3}$, $\mu = 2.167 \text{ mm}^{-1}$, $T = 100(2) \text{ K}$, 7063 reflections collected, 4889 unique ($R_{\text{int}} = 0.0604$), $R1 = 0.0789$, $wR2 = 0.2124 [I > 2\sigma(I)]$.

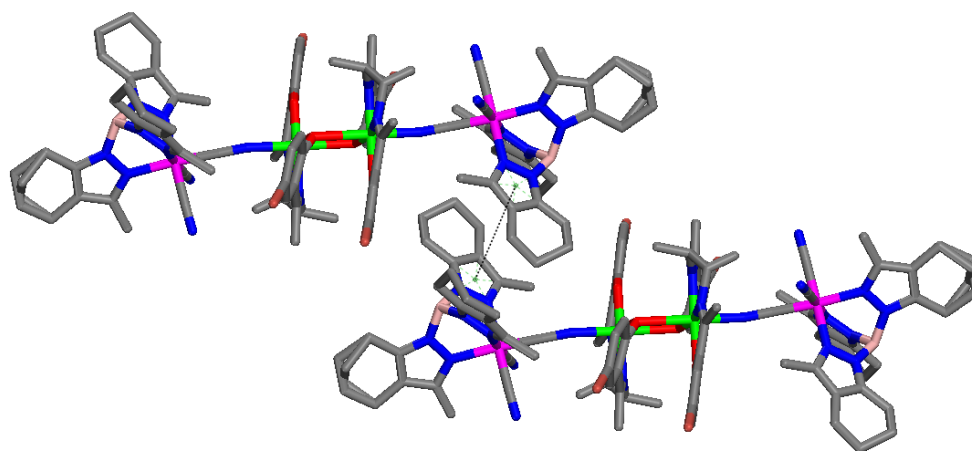


Fig. S1. The crystal packing diagram of **1** showing negligible intermolecular contacts with a centroid distance between pyrazole rings of 4.598 Å (dotted line).

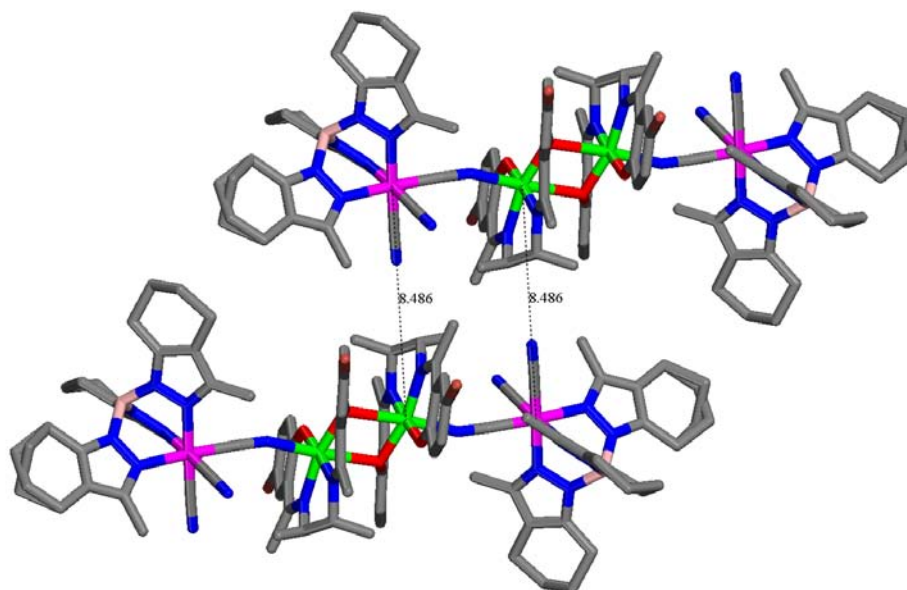


Fig. S2. Extended view **1** with the shortest intermolecular Fe-Mn distance of 8.486 Å.

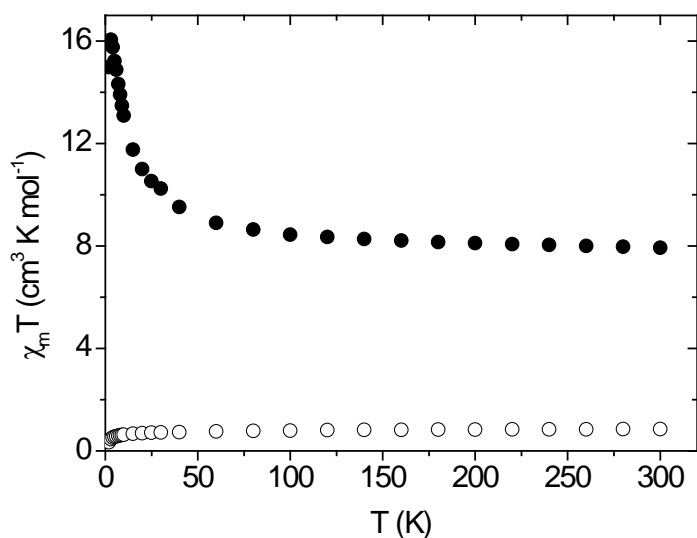


Fig. S3. Plots of $\chi_m T$ versus T . Closed and open circles represent the magnetic data for **1** and two Fe tricyanide units, respectively.

We subtracted the contribution of the Fe tricyanide units from the original data to generate the modified $\chi_m T$ curve. The subtraction procedure did not give substantially different $\chi_m T$ values from the raw data. The fitting of the modified data with the tetrameric model gave similar J values. This implies that the lower symmetry of the complex might be effectively quenching the orbital contribution. We used the same g value for Fe and Mn to get a reasonable result and the obtained g value is 2.13. It was not necessary to consider paramagnetic impurities in this system.

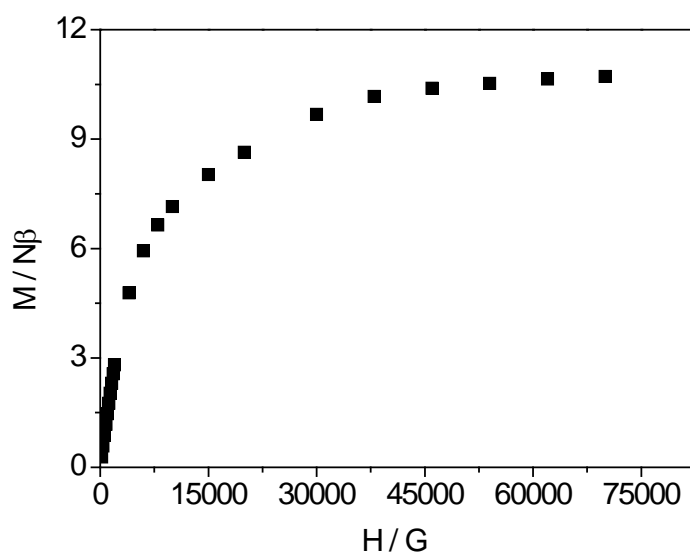


Fig. S4. Plot of M versus H of **1**.

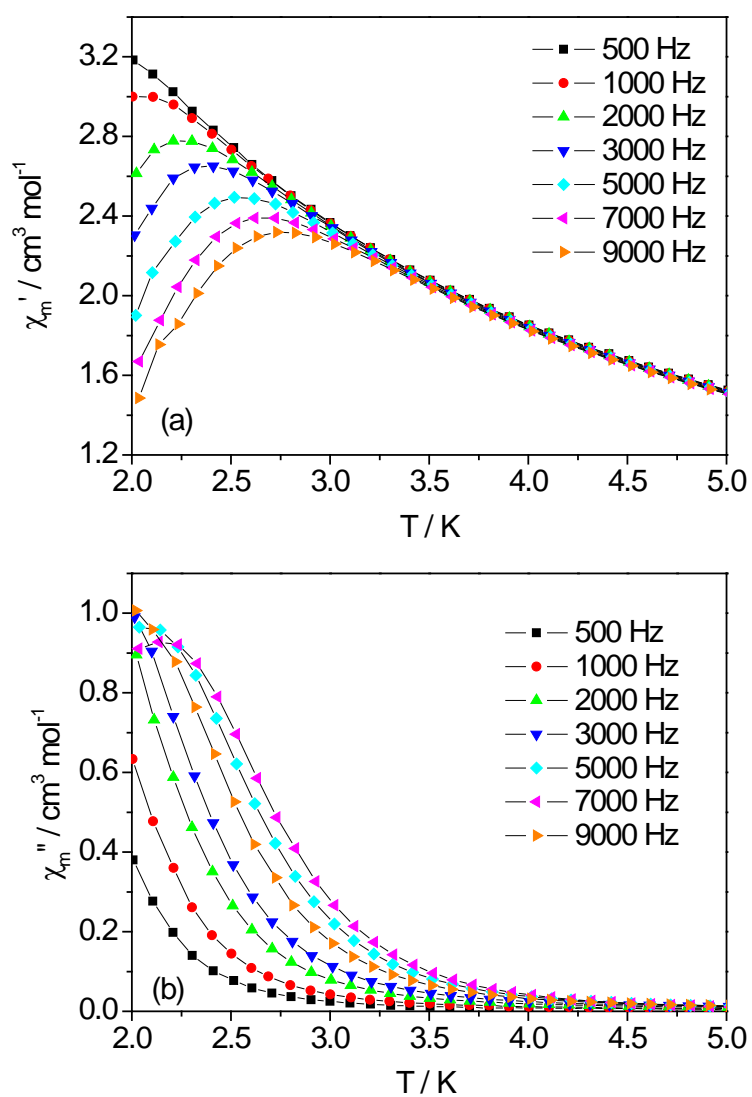


Fig. S5. Plots of (a) χ_m' and (b) χ_m'' versus T for **1** at zero dc field, an ac field of 5 G, and several frequencies.

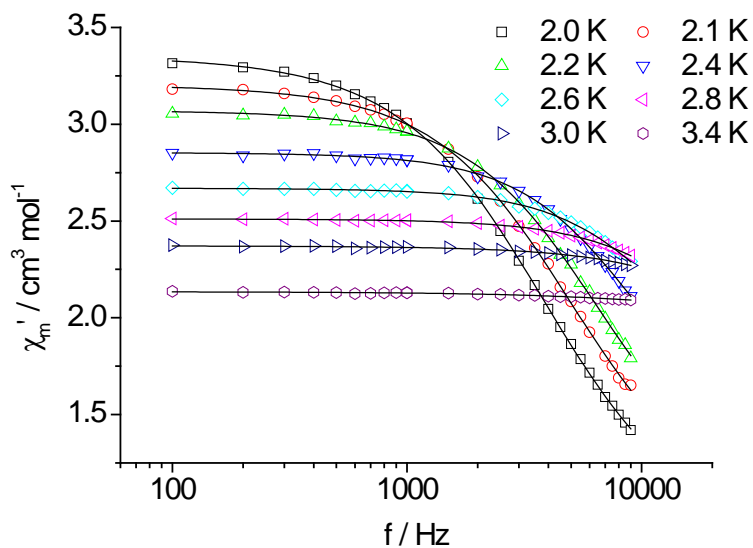


Fig. S6. Frequency dependences of χ'_m for **1** measured at $H_{dc} = 0$ G and $H_{ac} = 5$ G. The solid lines indicate appropriate theoretical fits to the data.

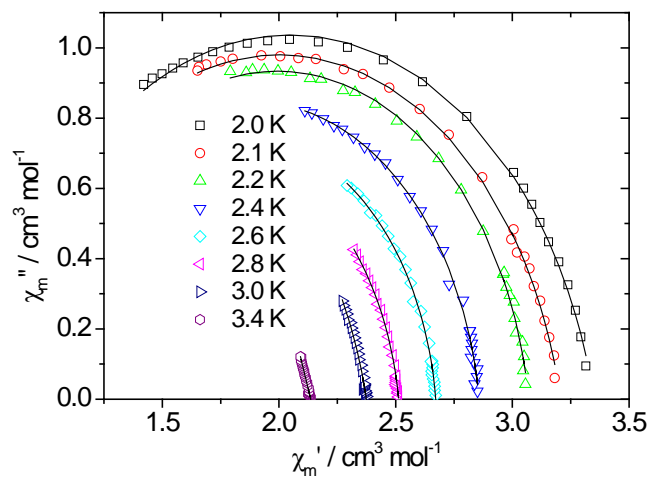


Fig. S7. Cole-Cole plots for **1**. The solid lines indicate appropriate theoretical fits to the data.

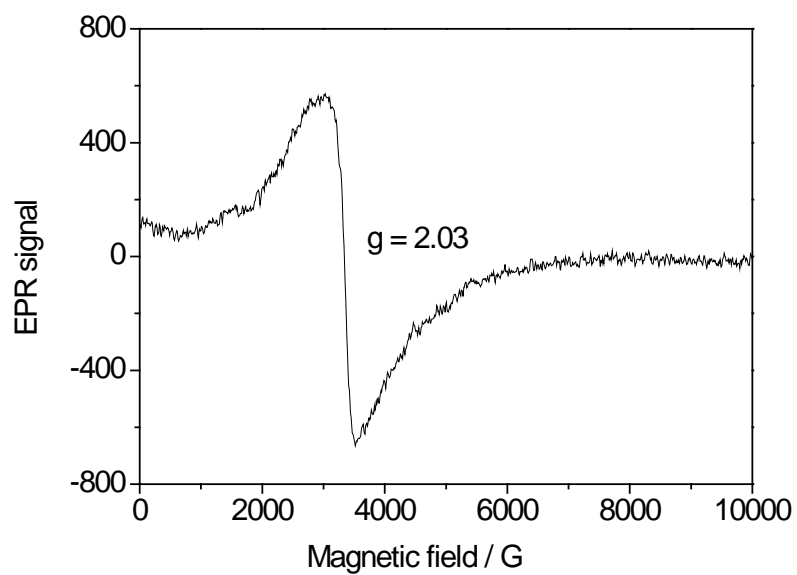


Fig. S8. EPR spectrum for the Fe tricyanide precursor at room temperature. The slight asymmetry in the signal indicates more complex behavior (g asymmetry) although we showed the isotropic single g value.